


Original Research Article

Optimizing retinal vessel visualization using multi-exposure fusion and adaptive contrast enhancement for improved diagnostic imaging

Cristian-Dragoş Obreja *

Department of Materials and Environmental Engineering, Faculty of Engineering, “Dunarea de Jos” University of Galati, 47 Domneasca, 800008 Galati, Romania

*Corresponding author email: cristian.obreja@ugal.ro

	International Archives of Integrated Medicine, Vol. 11, Issue 11, November, 2024. Available online at http://iaimjournal.com/
	ISSN: 2394-0026 (P) ISSN: 2394-0034 (O)
	Received on: 2-11-2024 Accepted on: 14-11-2024 Source of support: Nil Conflict of interest: None declared. Article is under Creative Common Attribution 4.0 International DOI: 10.5281/zenodo.14237852
How to cite this article: Cristian-Dragoş Obreja. Optimizing retinal vessel visualization using multi-exposure fusion and adaptive contrast enhancement for improved diagnostic imaging. Int. Arch. Integr. Med., 2024; 11(11): 1-10.	

Abstract

This study presents a multi-exposed fusion algorithm aimed at enhancing the quality of retinal images captured under variable illumination conditions. Retinal imaging devices frequently struggle with inconsistent lighting, which can lead to low-contrast images where critical vascular details may be lost. The proposed algorithm combines multiple exposures, preserving the best features from each - improving both clarity and detail. Using the database of 40 retinal images, the method evaluates image quality through the structural similarity index measure (SSIM). Results indicate high structural similarity between fused images and input images across different illumination levels, with SSIM values above 0.9 for medium and high exposure. Furthermore, incorporating Contrast-Limited Adaptive Histogram Equalization (CLAHE) enhances contrast, facilitating clearer vessel visualization against the background. The improved contrast and detail retention achieved by the algorithm support accurate retinal vessel analysis, which is crucial in diagnosing conditions like diabetic retinopathy and glaucoma. This approach provides a robust, enhanced imaging solution for medical diagnostics, significantly improving readability and reliability in retinal assessments.

Key words

Multi-exposure fusion, Retinal imaging, Contrast enhancement, SSIM, CLAHE, Blood vessel visualization, Diabetic retinopathy.

Introduction

Imaging equipment, which includes fundus cameras, OCT scanners, and fluorescein angiography devices, faces challenges in capturing high-quality images with optimal brightness and contrast [1]. These devices depend on proper lighting, exposure settings, and sensor sensitivity to capture fine retinal details. However, achieving uniform illumination is difficult due to inherent limitations, often resulting in low contrast between retinal vessels and surrounding tissues. This can cause over exposed or under exposed areas, leading to a loss of critical details [2-6]. Image quality may also degrade due to patient movement, pupil dilation variations, cataracts, and other ocular conditions. To address these issues, advanced post-processing techniques like multi-exposure fusion algorithms are necessary [7-9]. These algorithms combine images taken at varying exposure levels to produce a single, enhanced image, preserving the best aspects of both dark and bright regions. This approach makes subtle structures, such as small retinal vessels, more visible, improving diagnostic accuracy. Enhanced luminosity and contrast benefit subsequent image analysis steps like segmentation and edge detection, crucial for accurately isolating blood vessels. By improving image clarity and detail, multi-exposure fusion supports better monitoring and diagnosis of conditions such as diabetic retinopathy, glaucoma, and hypertension, contributing to improved patient care in ophthalmology [8-14].

Materials and methods

Data base and Workflow

DRIVE is one of the most popular databases related to the analysis of images in the human retina, specially conceived to support research activities concerning the automatic segmentation and analysis of vessels in images of the retina. It was developed by the Image Sciences Institute of the Utrecht University in the Netherlands, based

on a diabetic retinopathy screening program. In this work, the used dataset involves color fundus images taken for a total of 40. Images in this dataset had been taken from the Canon CR5 non-mydratic 3CCD camera with a field view of 45 degree images. Each image has a resolution of 768×584 pixels. These images contain both normal and pathological cases to provide a comprehensive test set for evaluating algorithms. For the ground truth comparison, manual segmentations of retinal vessels are also provided in the DRIVE database by two independent human observers [15]. The first one was used as a reference standard while the second was included for comparative analysis, where by the researchers could compare the performance of their algorithms to that of a human. Owing to the high quality of images and detailed annotation, the present database is rather useful in the development and testing of machine learning models and image processing algorithms directed at vessel segmentation, edge detection, and similar tasks.

Multi-exposed fusion algorithm

Multi-exposure fusion algorithms merge several images of the same scene taken with different exposures into one well-exposed image that captures from each input the best details. Basically, it works by first capturing multiple shots of a scene using different exposures - from under to over exposure. Then, for every image, weight maps will be computed, emphasizing those regions that contain desirable features such as good exposure, high contrast, and vivid colors. These images and their weight maps are decomposed into multi-level pyramids, Laplacian pyramids of the images, and Gaussian pyramids of the weight maps, to capture the details in different resolutions [12-14]. Then, at each level in the pyramids, images undergo a weighted blend through their weight maps; this ensures that the best portions of each image are retained.

Finally, the pyramid levels of the fused image undergo up sampling and addition to reconstruct the final image [16-19]. In order to enhance visual quality, post-processing steps such as tone mapping and noise reduction are done to widen the dynamic range through a seamless, well-balanced image preserving details, brightness, and color from all input exposures [19, 20].

Multi-exposure fusion enhances the algorithm of detecting retinal vessels by merging images taken under different exposures into one well-balanced image. This technique maintains the best details of both images with the enhancement of contrast and visibility of faint blood vessels and the reduction of noise and artifacts. Given that well-exposed regions are highlighted and that vessel clarity is enhanced in the resulting fused image, it provides a better view of the retina for more accurate detection and analysis of the retinal vessels. Indeed, this fact is critical in the diagnosis of several pathologies such as diabetic retinopathy, whose diagnoses depend on the precise visualization of blood vessels [18-20].

Weight Map Generation

One of the steps in multi-exposure image fusion involves the generation of weight maps to help with determining how much each particular image should contribute. The function computes three weights for every image: contrast weight, saturation weight, and well-exposedness weight. The contrast weight is obtained from the local contrast of each image, putting more emphasis on those regions where the changes in intensity are larger. These can be edges or detailed regions [13]. It enhances the sharpness and clarity of the fused image and ensures that well-defined areas receive higher priorities. Saturation weight is based on the color saturation of the image and favors regions of an image with more vivid colors. Generally, higher saturation corresponds to the most visually appealing and informative parts of the image; thus, these areas will be prioritized in the fusion process [16].

Finally, the well-exposedness weight measures how well each pixel is exposed, preferring

neither too dark nor too bright pixels. This calculates a Gaussian function evaluating the closeness of each pixel's intensity to an optimal mid-range value. It improves the regions with good exposure while constraining the contribution of over exposed or under exposed areas [16-18]. During the combination of these three weight maps, the fusion process can ensure that the best-exposed, most colorful, sharpest parts from each input image are retained by the final image.

Pyramid Decomposition

Since multi exposure fusion also relies largely on pyramid decomposition, images and their weight maps are represented at multiple resolutions. Pyramid decomposition breaks down the images into their respective Laplacian pyramids and the corresponding weight maps into Gaussian pyramids. Each image is decomposed using a Laplacian pyramid because it captures the details of the image at various resolutions; hence, the edges and textures at each scale can be isolated effectively. That is, finer details remain preserved toward the top of the pyramid, while coarser structures remain preserved further down the pyramid [20].

In parallel, for the weight maps, parallel Gaussian pyramid decomposition is adopted. The Gaussian pyramid creates a smoothed, progressively lower-resolution version of the weight map at each level. The smoothing helps in gradually blending the weight values derived during the weighting step and provides a more coherent influence across different image scales at the time of performing the fusion. By representing the images together with their weights at multiple levels, the pyramid decomposition provides a means for carrying out the blending process in a manner that respects both the fine detail and overall structure of the images [21].

This multi-resolution approach enables the fusion process to seamlessly combine images of varying sharpness and exposure, ensuring that every portion of the final image benefits from the best

possible representation of detail and clarity. For instance, fine textures and edges from the Laplacian image pyramids are combined with smoothly varying weight values from Gaussians, resulting in a more natural balance that is appropriate in the fused results. The pyramid decomposition will ensure that high-frequency details are not lost while retaining the overall smoothness during fusion so that the final image is both sharp and well-integrated throughout the exposures [21, 22].

Fusion of Pyramids

The fusion of pyramids is a key stage in the multi-exposure image fusion process, where the decomposed images and weight maps are combined to create a balanced and detailed final image. This is done at each level of the pyramid, utilizing a function which performs a weighted sum of the images based on the values in their corresponding weight maps. The weighted sum approach allows each image to contribute to the final result according to how favorable its attributes are at that particular resolution level. Smoothing and adjusting the properties through a Gaussian pyramid decomposition of the weight maps guides this process of blending by giving higher weights to areas of each image that are best exposed, highly contrasted, and richly colored [23].

If, for example, a region in one of the input images enjoys better contrast or is better exposed than its counterpart in another image, then this weight map will ensure that more attention is given to that particular region of interest during the fusion process. In scenes where edges are sharper, textures clearer, or exposure conditions superior, dominance of such regions at each pyramid level of the merge ensures greater contribution to the composite image. It then cascades this process of fusion at all levels of the pyramid, from the finest details to the coarser structures in the image, so that every aspect of the images – may be fine textures, or more general brightness and color balance is optimally combined into the final result [20-23].

By fusing the images with these weight maps, the appropriate sharpness and contrast from the well-defined regions, vibrancy from the saturated, and proper balance from the well-exposed parts maintain their properties in the fused image. This technique will ensure that the final image is seamless without any traces of transition between different regions, retaining all the best characteristics from each input image to deliver a rich, and well-balanced result [16]. For each level l , the fused pyramid level F^l is computed as a weighted sum of the Laplacian pyramid levels from all input images, adjusted by their respective weights. Mathematically, this is expressed as:

$$F^l = \frac{\sum_{i=1}^N W_i^l \cdot L_i^l}{\sum_{i=1}^N W_i^l + \epsilon}$$

where:

- N : The number of input images.
- W_i^l : The weight map for image i at level l .
- L_i^l : The Laplacian pyramid of image i at level l .
- ϵ : A small constant added to the denominator to prevent division by zero.

Reconstruction of the Fused Image

The final step in the multi-exposure fusion process is reconstructing the fused image, where all the combined data from each pyramid level is reassembled into a complete, detailed image. After blending the decomposed pyramids of the input images, we are rebuilding the image from its fused pyramid structure. This process starts from the lowest resolution level, working upwards to the highest. At each level, the image data is up sampled – meaning its resolution is increased to align with the next level [21-23].

Up sampling is critical because it allows the finer details and high-frequency components from the higher pyramid levels to integrate smoothly with the broader structures captured at lower levels. As each up sampled level is combined with the corresponding level in the pyramid, the details

are progressively restored, layering the image back together. This method ensures that both fine textures and general luminance and color gradients are preserved, creating smooth transitions across different parts of the image.

The end result is a reconstructed image that effectively combines the strengths of each input exposure, maintaining sharpness, appropriate exposure, and balanced color throughout [23]. This approach ensures that the final image retains the detailed elements captured by the Laplacian decomposition while benefiting from the smooth blending achieved during fusion. The reconstructed image looks natural and visually appealing, integrating the best features of each original image into a single, seamless output, free from issues like blurring or abrupt transitions. This reconstruction process ensures that the final image is rich in detail and depth, offering a dynamic and true representation of the original scenes [23].

Post-Processing (Tone Mapping and Noise Reduction)

Post-processing is one of the most important steps to refine the final fused image for display or any further use. Tone mapping remains the critical phenomenon during this step, where the intensity levels of an image are changed in such a way that general brightness and contrast become near to natural and balanced. Tone mapping becomes especially necessary when the image has high dynamic range – one with huge differences between the darkest and brightest areas [24-26]. The intensity values of the fused image have to be normalized to the input values within the displayable range so that the image may appear more consistent and detailed on standard screens. This transforms an image in such a way that details in both shadowed and bright areas are well preserved, without any part of the image being too dark or washed out.

Noise reduction is further applied as post-processing in enhancing the clarity of the final image through a bilateral filtering technique, which smooths the noisy image while preserving

edges and other important information. Noise will be filtered from this image using the *imblatfilt* function. Unlike traditional filters that blur edges, in bilateral filtering, the averaging of pixels is performed based on their spatial proximity and likeness in intensity. This will reduce random noise in such a way that it will maintain sharp edges and textures of the image.

This combination of mapping tone and reducing noise naturally sees that the merged image is natural, balanced-looking, clean, and clear. That is, the process of tone mapping optimizes the image while considering the best conditions for viewing. Noise reduction, on the other hand, clears the grainy artifacts that might have been introduced through earlier steps in image fusion. These steps together retouch the final output to be both visually attractive and technically appealing for viewing, printing, or further digital manipulation [25, 26]. This provides a high-quality image that is smooth, well-detailed, visually harmonious, and with a full range of tones and minimal noise.

Contrast-Limited Adaptive Histogram Equalization (CLAHE)

CLAHE, in short, indicates contrast-limited adaptive histogram equalization; this improves the original histogram equalization methods. Based on this improvement, the rationale was to avoid the over-enhancement of noise and other artifacts in homogeneous regions of the image. CLAHE performs the division of the image into small regions and then assists in applying histogram equalization in each tile independently [24]. This local adjustment increases the contrast in every region so that details may show more easily both in bright and dark areas.

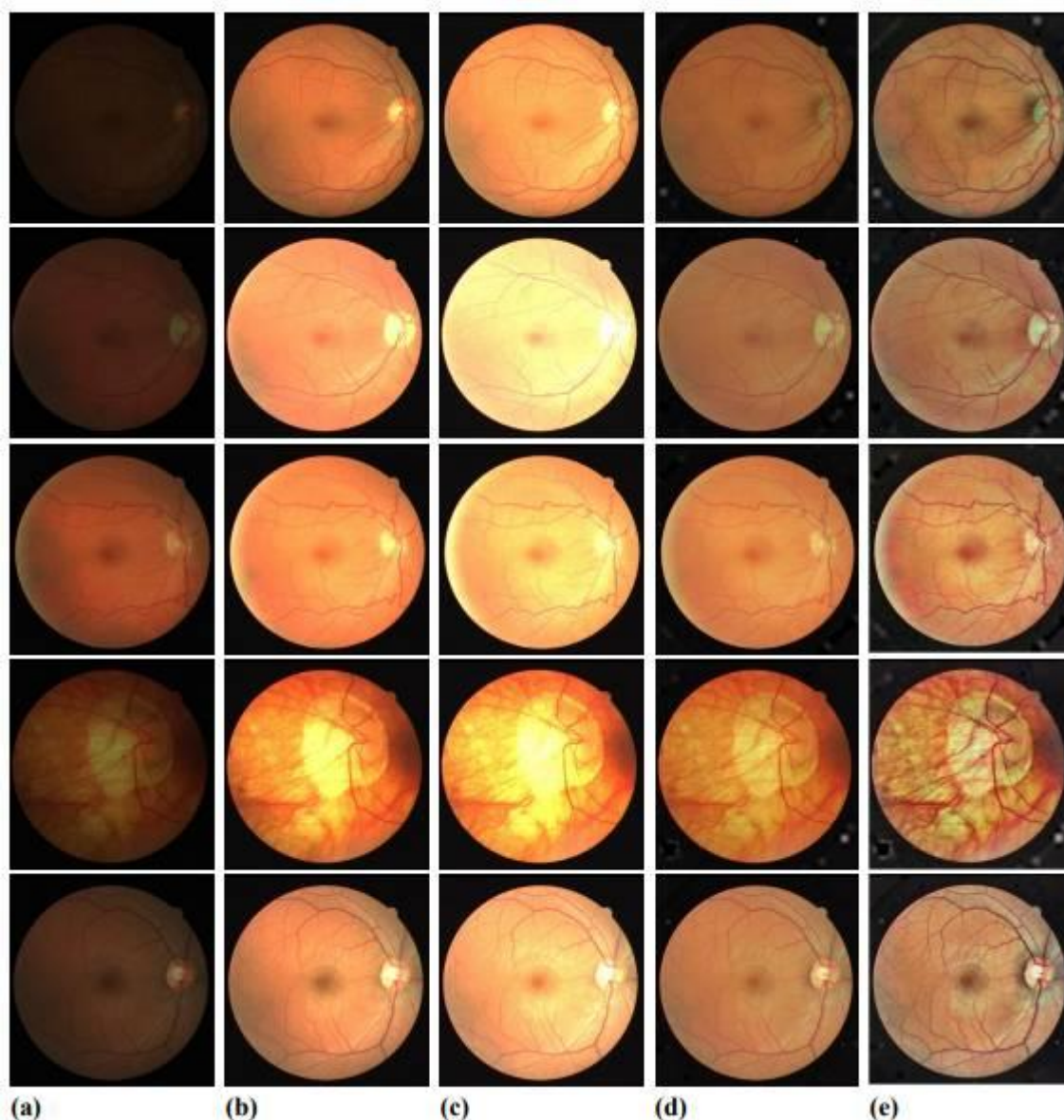
Once local equalization has been done for each of the tiles, CLAHE does a sort of blending of the tiles through bilinear interpolation in order to ensure smooth transitions across bordering tiles and to avoid artificial frontiers. A key feature of CLAHE, however, is that it applies a contrast clipping threshold - an upper limit on the height of the histogram of every tile. This avoids the

over-enhancement of regions that might otherwise lead to the amplification of unwanted noise [24, 25].

CLAHE can generate enhanced contrast images that also have a natural appearance with controlled limits on their distribution of pixel

intensities for preserving significant details in images. It can be used in a wide array of areas in medical imaging, remote sensing, and photography, where such detail enhancement would be very much needed to be preserved while there is a need for improvement in lightening the visibility [24].

Figure – 1: Examples of vascular map. (a) Input image with low exposure; (b) Input image with medium exposure; (c) Input image with high exposure; (d) Fused image (e) Fused image with CLAHE filter.



Performance evaluation

Structural Similarity Index Measure, is a perceptual metric for assessing image quality. Unlike simple pixel comparison metrics like Mean Squared Error (MSE) or Peak Signal-to-

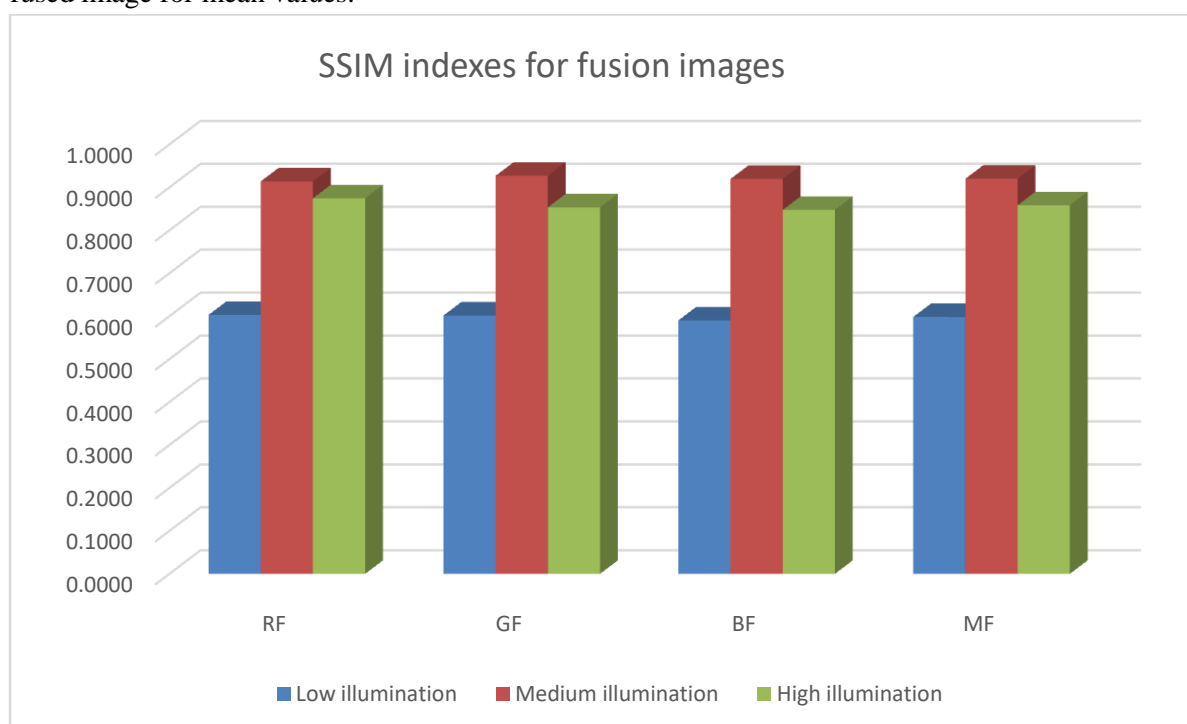
Noise Ratio (PSNR), SSIM considers changes in structural information, luminance, and contrast, making it particularly effective for measuring visual quality as perceived by the human eye [26-28].

The SSIM formula compares two images, x and y , typically in sliding windows, and is given by:

$$SSIM(x, y) = \frac{(2\mu_x\mu_y + C_1)(2\sigma_{xy} + C_2)}{(\mu_x^2 + \mu_y^2 + C_1)(\sigma_x^2 + \sigma_y^2 + C_2)}$$

where: μ_x and μ_y are the average intensities of images x and y , σ_x^2 and σ_y^2 are the variances, σ_{xy} is the covariance between x and y , C_1 and C_2 are small constants to stabilize division, especially when the denominator is closet o zero [27, 28].

Figure – 2: SSIM values for: (a) input image and fused image for red channel; (b) input image and fused image for green channel; (c) input image and fused image for blue channel; (d) input image and fused image for mean values.



In **Figure – 2**, a comparison between SSIM values of fused images and the three input images, affected by different levels of illumination. In the forth group the mean SSIM values, calculated between the fused images and the three input images is presented. In the first three groups the SSIM values calculated between the red channels (RF), green channels (GF) and blue channels (BF) of the input and fused images are presented. Each group has three columns, for low, medium and high illumination.

Results and Discussion

To assess the performance of the proposed fusion algorithm compared with the original images, the structural similarity index measure was conducted on 40 randomly selected color retinal images, each with three levels of illumination. **Figure – 1** illustrates examples of vascular maps generated using the multi-exposed fusion algorithm, those generated using CLAHE over the fused images, and the three images used as input information for the fusion method.

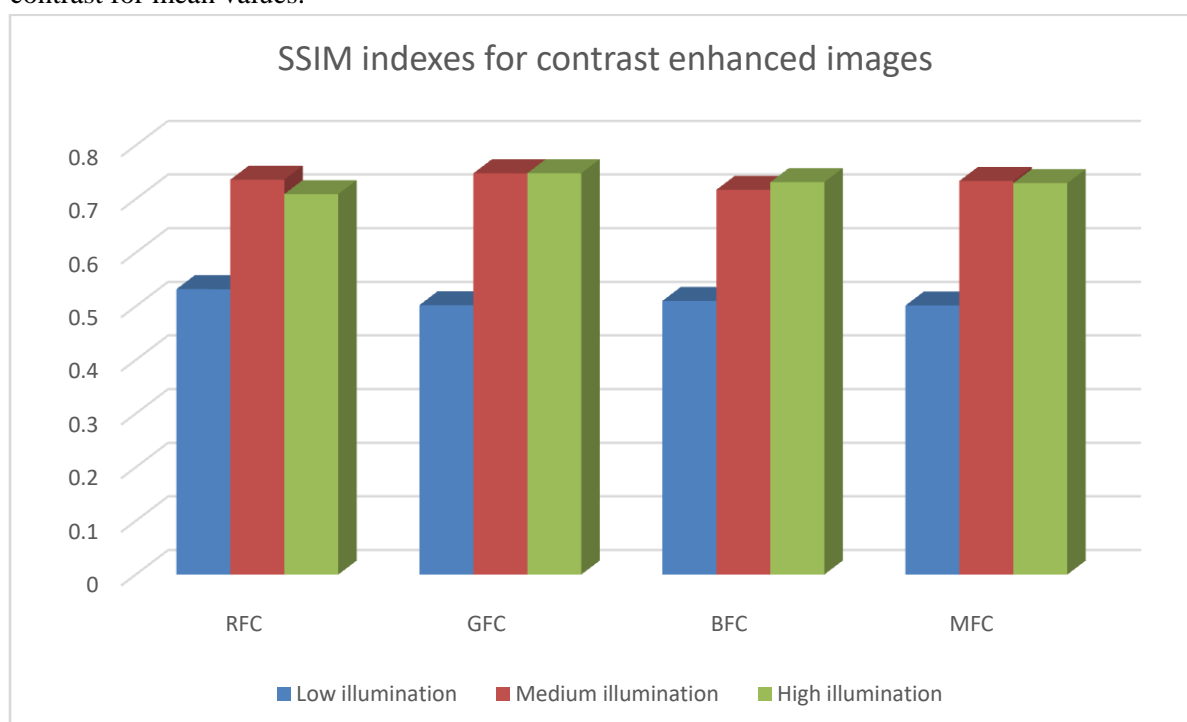
Similarly, in **Figure - 3**, the SSIM values of fused and input images is presented, for the mean, red channel, green channel and blue channel are presented.

The study focuses on improving retinal image quality for diagnostic purposes by addressing the challenge of illumination variability. Images captured under different illumination levels can impact visibility and quality, which are crucial for accurate analysis of vascular structures in the retina. The main advantage of the multi-exposed

fusion algorithm is its ability to combine images taken at different exposure levels, which results in a single, high-quality image with enhanced visibility of retinal structures. This approach mitigates the impact of illumination variability, which can obscure details in individual low, medium, or high-exposure images. Also,

enhanced SSIM values indicate that the algorithm can provide more consistent structural similarity, which is critical for medical image diagnostics, particularly in vascular mapping of retinal images. The contrast-limited adaptive histogram equalization filter further enhances the contrast, potentially aiding in clinical readability.

Figure – 3: SSIM values for: (a) input image and fused image with enhanced contrast for red channel; (b) input image and fused image with enhanced contrast for green channel; (c) input image and fused image with enhanced contrast for blue channel; (d) input image and fused image with enhanced contrast for mean values.



As we can see from **Figure - 2**, the SSIM values computed, show that there is a high similarity between the fused image and the original input images, especially for the medium and high illumination images. In these cases the SSIM values for the mean values, as well as for the red, green and blue channels values is over 0.9. Furthermore, for the CLAHE enhanced images, we can see the structural similarity index values are very high, in particular for the medium and high illumination.

According to the SSIM values the multi-exposed fusion algorithm keeps the retinal vascular tree characteristics and improves their visibility. Also,

visually, it improves the blood vessel edge visibility compared with the background.

Furthermore, the fused images improved with CLAHE, have an even higher contrast between the foreground and the background, making the vascular tree easier to differentiate against the background. This is done by making the blood vessels edges more visible against the background, with a higher drop of pixel intensity between the vessel and the neighbouring area.

Conclusion

In summary, the multi-exposed fusion algorithm significantly improves retinal image quality by merging images taken at various exposure levels,

allowing for enhanced visibility of retinal vessels even under inconsistent illumination. SSIM evaluations confirm that fused images closely resemble the input images, especially under medium and high illumination, with similarity values frequently above 0.9 for individual color channels and mean values. Additionally, the use of Contrast-Limited Adaptive Histogram Equalization (CLAHE) further heightens contrast, aiding in clearer differentiation of blood vessels from the background. This combined approach not only preserves essential vascular details but also improves contrast, which is critical for diagnosing conditions like diabetic retinopathy. By enhancing both visibility and contrast, the algorithm provides a powerful tool for accurate retinal analysis, supporting reliable diagnostics.

References

1. Abramoff M.D., Garvin M.K., Sonka M. Retinal imaging and image analysis. *IEEE Rev. Biomed. Eng.*, 2010; 3: 169-208.
2. Zhang J, Dashtbozorg B, Bekkers E, Pluim JP, Duits R, Ter Haar Romeny BM. Robust Retinal Vessel Segmentation via Locally Adaptive Derivative Frames in Orientation Scores. *IEEE Trans Med Imaging*, 2016; 35(12): 2631-2644.
3. Riaz T., Akram M., Laila U., Khalil M.T., Zainab R., Iftikhar M., Ozdemir F.A., Sołowski G., Alinia-Ahandani E., Altable M., Egbuna C., Sfera A., Adnan M., Parmar P. The analysis of retinal blood vessels and systemic diseases includes the relationship between retinal blood vessels and myocardial infarction (heart disease), and retinal blood vessels and cerebrovascular diseases. *IAIM*, 2023; 10(11): 61-68.
4. Lakshminarayanan V, Kheradfallah H, Sarkar A, Jothi Balaji J., Automated Detection and Diagnosis of Diabetic Retinopathy: A Comprehensive Survey. *J Imaging*, 2021; 7(9): 165.
5. Buades A, Lisani JL, Martorell O. Efficient joint noise removal and multi exposure fusion. *PloS One*, 2022 Mar 25; 17(3): e0265464. doi: 10.1371/journal.pone.0265464.
6. Buades A., Coll B., Morel J.M. A non-local algorithm for image denoising. In: *Proceedings of the IEEE Conf. Comput. Vision Pattern Recognit. (CVPR)*, 2005; 60-65.
7. Wang X., Sun Z., Zhang Q., Fang Y., Ma L., Wang S., Kwong S.T. Multi-Exposure Decomposition-Fusion Model for High Dynamic Range Image Saliency Detection. *IEEE Transactions on Circuits and Systems for Video Technology*, 2020; 30: 4409-4420.
8. Dabov K., Foi A., Katkovnik V., Egiazarian K. Image denoising by sparse 3-D transform-domain collaborative filtering. *IEEE Trans. Image Process.*, 2007; 16(8): 2080-2095.
9. Saffarzadeh VM, Osareh A, Shadgar B. Vessel Segmentation in Retinal Images Using Multi-scale Line Operator and K-Means Clustering. *Journal of Medical Signals and Sensors*, 2014; 4(2): 122-129.
10. Grisan E, Foracchia M, Ruggeri A. A novel method for the automatic grading of retinal vessel tortuosity. *IEEE Trans Med Imaging*, 2008 Mar; 27(3): 310-9.
11. He K., Zhang X., Ren S., Sun J. Deep residual learning for image recognition. *Proceedings of the IEEE Conf. Comput. Vision Pattern Recognit. (CVPR)*, 2016; 770-778.
12. Li M, Ma Z, Liu C, Zhang G, Han Z. Robust Retinal Blood Vessel Segmentation Based on Reinforcement Local Descriptions. *Biomed Res Int.*, 2017; 2017: 2028946. doi: 10.1155/2017/2028946.
13. Xu K., Wang Q., Xiao H., Liu K. Multi-Exposure Image Fusion Algorithm Based on Improved Weight Function. *Frontiers in Neurorobotics*, 2022; 16: 846580.

- <https://doi.org/10.3389/fnbot.2022.846580>
14. Y. Li, M. Liu and K. Han. Overview of Multi-Exposure Image Fusion, 2021 International Conference on Electronic Communications, Internet of Things and Big Data (ICEIB), Yilan County, Taiwan, 2021, pp. 196-198.
 15. Digital Retinal Images for Vessel Extraction (Image Sciences Institute, University Medical Center Utrecht), <http://www.isi.uu.nl/Research/Databases/DRIVE/> (2004).
 16. Chen X., Hu Y., Xu X., Wang J. Multi-exposure fusion using edge-preserving decomposition and saliency-weighted features. *IEEE Access*, 2019; 7: 54108-54117.
 17. Qi G., Chang L., Luo Y., Chen Y., Zhu Z., Wang S. A Precise Multi-Exposure Image Fusion Method Based on Low-level Features. *Sensors*, 2020; 20: 1597. <https://doi.org/10.3390/s20061597>
 18. Nagpal D., Alsubaie N., Soufiene B.O., Alqahtani M.S., Abbas M., Almohiy H.M. Automatic Detection of Diabetic Hypertensive Retinopathy in Fundus Images Using Transfer Learning. *Appl. Sci.*, 2023; 13: 4695. <https://doi.org/10.3390/app13084695>
 19. Wang S., Chen Y., Yi Z. A Multi-Scale Attention Fusion Network for Retinal Vessel Segmentation. *Appl. Sci.*, 2024; 14: 2955. <https://doi.org/10.3390/app14072955>
 20. Surya S., Muthukumaravel A. Adaptive Sailfish Optimization-Contrast Limited Adaptive Histogram Equalization (ASFO-CLAHE) for Hyperparameter Tuning in Image Enhancement. In: Joseph, F.J.J., Balas, V.E., Rajest, S.S., Regin, R. (eds) *Computational Intelligence for Clinical Diagnosis*, 2023.
 21. Dissopa J., Kansomkeat S., Intajag S. Enhance Contrast and Balance Color of Retinal Image. *Symmetry*, 2021; 13: 2089.
 22. J. Lei, J. Li, J. Liu, S. Zhou, Q. Zhang and N. K. Kasabov. GALFusion: Multi-Exposure Image Fusion via a Global-Local Aggregation Learning Network. *IEEE Transactions on Instrumentation and Measurement*, 2023; 72: 1-15.
 23. Miri M.S., Mahloojifar A. Retinal image analysis using curvelet transform and multistructure elements morphology by reconstruction. *IEEE Trans. Biomed. Eng.*, 2011; 58(5): 1183-1192.
 24. Haddadi Y.R., Mansouri B., Khodja F.Z.I. A novel medical image enhancement algorithm based on CLAHE and pelican optimization. *Multimed Tools Appl*, 2024. <https://doi.org/10.1007/s11042-024-19070-6>
 25. Ravishankar S., Jain A., Mittal A. Automated feature extraction for early detection of diabetic retinopathy in retinal images. In: *Proceedings of the IEEE Conf. Comput. Vision Pattern Recognit. (CVPR)*, 2009; 210-215.
 26. Osorio F., Vallejos R., Barraza W., et al. Statistical estimation of the structural similarity index for image quality assessment. *SIViP*, 2022; 16: 1035-1042.
 27. Wang Z., Bovik A.C., Sheikh H.R., Simoncelli E.P. Image quality assessment: From error visibility to structural similarity. *IEEE Trans. Image Process.*, 2004; 13(4): 600-612.
 28. Cheng J., Wang Z. Improved structural similarity index for image quality assessment, *Journal of Computer Science*, 2014; 10(2): 353-360.